Influence of Cutting Conditions on Surface Integrity after Progressive Grinding of Blade Roots from Inconel 713LC

J. Čapek [1], K. Kolařík [1,a], Z. Pitrmuc [2], N. Ganev [1], L. Beránek [2], K. Trojan [1], J. Kyncl [2], J. Šimota [2]

[1] *Department of Solid State Engineering, Faculty of Nuclear Sciences and Physical Engineering, Czech Technical University in Prague, Trojanova 13, 120 00 Prague 2, Czech Republic*

[2] *Department of Machining, Process Planning and Metrology, Faculty of Mechanical Engineering, Czech Technical University in Prague, Technická 4, 166 07 Prague 6, Czech Republic*

[a] *kamil.kolarik@email.cz*

Abstract: The goal of this article is to describe changes of properties after progressive grinding of blade roots from Inconel 713LC. Especially, surface residual stresses were studied as a function of different grinding conditions and microstructure of bulk material. Residual stresses of surface layers were determined by using X-ray diffraction techniques.

Keywords: grinding; blade root; Inconel 713LC; residual stresses; cracks.

1 Introduction

Nickel-based superalloys are often used in automotive and aerospace industry as turbine blades for its excellent properties. Nevertheless, very stringent requirements on surface integrity specifically, residual stresses (RS) and microstructure are required, especially for blade roots because of its anchoring [1] and for service life under dynamic loads [2].

Therefore, the suitable selection of grinding conditions and adequate cooling are very important to prevent grinding burns. Otherwise, "thermal" RS are created due to stronger influence of accumulated heat more than the impact of plastic deformation. These unfavorable RS can result in crack initialization and its further propagation. Service life is not limited only by mechanical and thermal influences but also by the microstructure of the bulk material. The particles of ceramic inclusions, which can form in the material, are very hard and brittle; therefore, potential areas of the initialization of cracks are created by casting or ensuing solidification [3].

Using X-ray diffraction (XRD) techniques, the area with accumulation of unfavorable tensile RS of γ and γ' phases on a macroscale can be localized. Since the precipitates (γ' phase) are too hard to be plastically deformed, the local strain is very heterogeneous on a microscale – in the matrix channels, i.e. γ phase [4].

2 Experiment

The tested samples (blades) were made from nickel-based superalloy Inconel 713LC. The nominal chemical composition (in wt.%) of the as-cast samples was as follows: 12.0 Cr, 5.7 Al, 4.6 Mo, 2.0 Nb, 0.7 Ti, 0.2 Fe, 0.1 Zr, 0.08 Co, 0.05 C, 0.013 B and balance of Ni.

Surfaces of both sides, namely A (ground after wheel dressing) and B (without wheel dressing), of turbine blade roots with dimension 52 × 15 mm^2 were face ground. Further research will focus on the selection of grinding conditions for profile grinding. The grinding conditions were as followed: cutting speed v_c = 20 and 35 m/s, feed f = 450 and 600 mm/min, number of cuts N = 2 and 3, and final depth of cut (finishing) a_p = 0.05 and 0.07 mm. Together, 11 combinations of grinding conditions were used. Grinding wheel marked as *560038 STRATO ULTRA SU33A 542 GG 11 VB1* with dimensions 500×20×203.2 mm^3 was used. Grinding wheel is based on aluminum oxide grains a high porosity bond, suitable for creep feed grinding and grinding of blade roots.

Cooling fluid *Quakercool 710 LF* was used in concentration of 5 %. Cooling system enabled to bring enough amount fluid through tangential nozzle under the pressure of 10 bar.

Using Design of experiment, 3 areas were analyzed by XRD on each side of root, namely *I, II, III* and *IV, V, VI* on the side A and B, respectively, see Fig. 1. Longitudinal direction was parallel to the grinding direction and perpendicular to the axis of blades, see Fig. 1.

PROTO iXRD COMBO diffractometer in ω-goniometer set-up was used to measure lattice deformations using manganese radiation. The diffraction lines *{311}* of γ and γ' phases were measured in order to obtain macroscopic residual stresses [4]. Rachinger's method and Absolute peak method were used for determination of the diffraction angles $2\theta^{311}$ of the diffraction lines $K\alpha_1$. X-ray elastic constants $½s_2$ = 6.57 TPa^{-1}, s_1 = –1.56 TPa^{-1} for the residual stress determination using $\sin^2\psi$ method were calculated from components of stiffness tensor (C_{11} = 234.6 GPa; C_{12} = 145.4 GPa; C_{44} = 126.2 GPa) using Hill elastic model [5]. The cylinder collimator with Ø 2 mm was inserted into the primary beam path. The average value of the penetration depth of manganese radiation into the nickel-based material was approx. 4–5 μm [6].

In accordance with standard ČSN EN ISO 3452-1, the capillary tests were performed. Surface macro-etching was employed to reveal grain size and orientation obtained during casting. Also differentiation of intercrystalline and transcrystalline cracks was enabled. Metallographic samples were prepared in areas of capillary indications. Metallographic cross-sections were observed both in polished and etched (Marble's) condition.

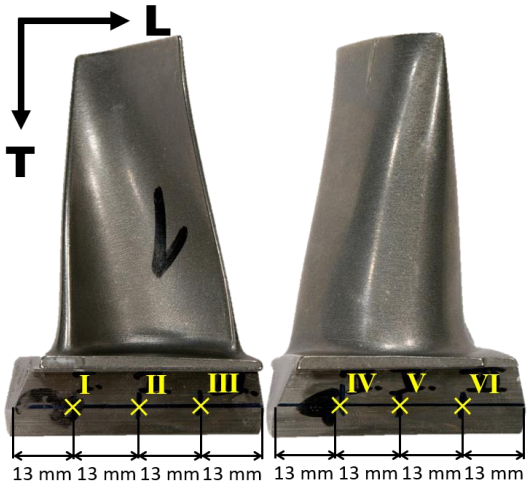

Fig. 1: Experimental sample (blade) with marked analyzed areas *I-III* and *IV-VI* on the side of root A and B, respectively.

3 Results and discussions

3.1 Microstructure and defectoscopy

Measured blade roots had homogenous values of RS on the ground surfaces areas *I-III* or *IV-VI* except for the roots which are depicted in Figs. 2-4. For the purpose of finding the reason of inequalities of these RS, the capillary tests, the metallographic cross sections and electro-etching for microstructure visibility were performed, see Figs. 5-8.

On the surface of several blade roots, the grinding burns were found, see Fig. 5. The grinding burns resulted in decrease of compressive RS values which are depicted in Fig. 2. The grinding burns were caused by insufficient cooling during grinding and probably by grain size and its orientation. The grinding burns were primarily detected on the edges of roots, as a result of a smaller amount of material for heat distribution[1], see Fig. 5. The anisotropy in polycrystalline samples is generally reduced more in comparison with single crystal, because of the distribution of crystal orientation. It means that in the case of coarse-grained material, there may be a grain which is oriented in a direction with smaller thermal conductivity parallel to the heat flow [7]. These grains may cause grinding burns.

[1] The thermal conductivity of Inconel is approx. 4× smaller in comparison with steel.

The sharp decrease of compressive RS on the surfaces for several blades was explained by metallographic cross sections obtained by capillary test through which, the cracks were found, see Figs. 3, 6 and 7. Regardless of the compressive RS in the surface layer 4-5 microns thick of ground roots, it is possible to expect that there are tensile RS in the deeper subsurface layers [8]. These RS have a negative effect on the functional characteristics of the blade roots and probably could cause cracks.

The rest of inhomogeneity were probably caused by coarse-grained microstructure of bulk material, see Figs. 4 and 8, which enables to predict that slip directions of several grains are parallel to the primary grinding force. Therefore, even smaller force could cause the slip and thereby smaller compressive RS are determined.

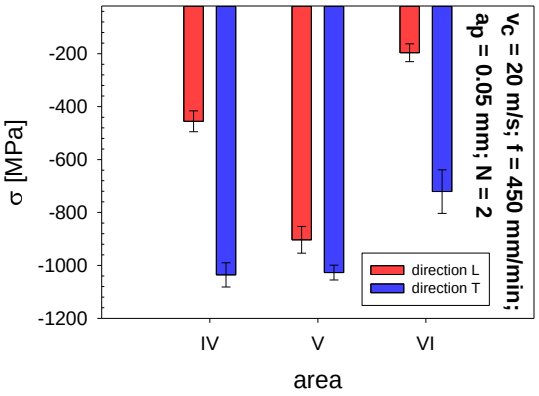

Fig. 2: Distribution of RS on the surface of the side B affected by grinding burns.

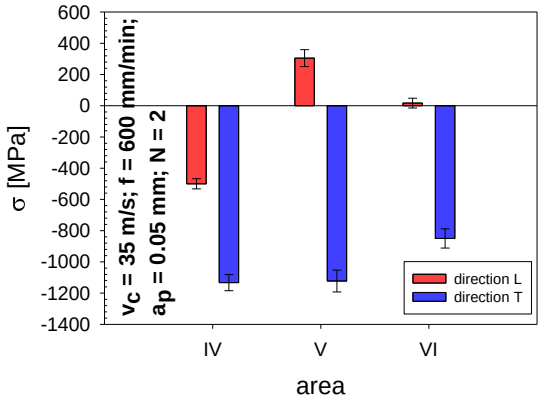

Fig. 3: Distribution of RS on the surface of the side B affected by presence of crack.

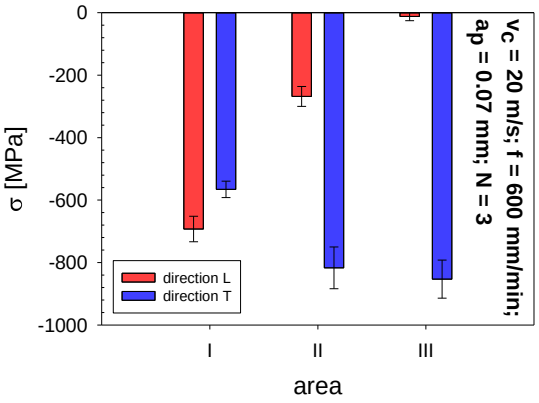

Fig. 4: Distribution of RS on the surface of the side A affected by coarse-grained bulk material.

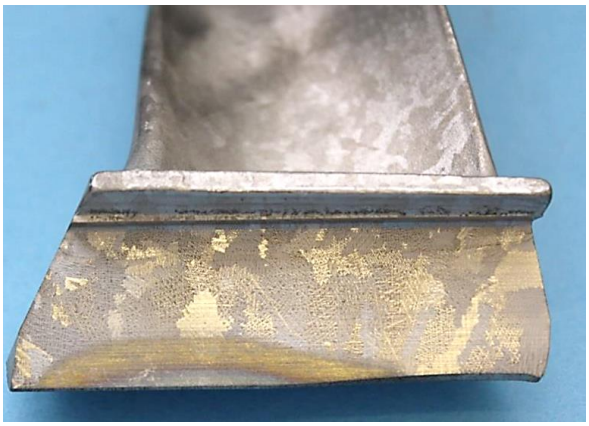

Fig. 5: Root surface of selected blade with the grinding burn.

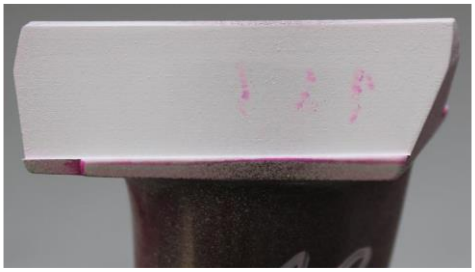

Fig. 6: Blade root with line indications of defects determined by capillary testing.

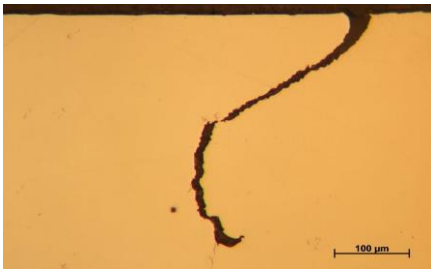

Fig. 7: Metallographic cross section of the line indication (crack) from Fig. 6.

Fig. 8: Fine-grained and coarse-grained microstructure of bulk material of selected samples.

3.2 Influence of grinding conditions

For the purpose to find the RS dependence on the grinding conditions, RS were averaged from three areas on each side of blade roots separately, see Tab. 1. Surface RS of various grinding conditions obtained by XRD are depicted in Figs. 9-11.

The values of RS depending on the final depth of cut a_p are in Fig. 9. A clear trend for both the analyzed sides and directions is observed, specifically, compressive RS increased in most cases with the depth of the cut increased. Greater plastic deformation (hardening) of material increased of mentioned RS in the surface layer 4-5 microns in thickness.

With increasing cutting speed v_c, the values of compressive RS had an increasing trend too, see Fig. 10. Greater hardening of ground surface was probably the reason of this trend.

Finally, with increasing number of cut[2], the compressive RS were higher. Various values of hardening were caused by different depths of cut after roughing.

From Tab. 1, it is possible to state that RS were for all the samples higher on the side B in comparison with RS on the side A in the transversal direction *T*, i.e. direction perpendicular to the grinding direction. In this case, the different values of RS were caused by wheel dressing.

According to the general assumptions of grinding theory [8], higher depth of final cut, faster cutting speed lead to greater increase of the material temperature which leads to tensile RS. The results of this article dealt with thin surface layer of compressive RS are inconsistent with the mentioned grinding theory. Nevertheless, with increasing of the subsurface depth, the tensile RS are predicted to the detriment of compressive RS.

Tab. 1: The average values of RS depending on grinding conditions.

Grinding conditions				**side A**				**side B**			
v_c [m/s]	f [mm/min]	N [-]	a_p [mm]	$\langle\sigma_L\rangle$ [MPa]	$\Delta\sigma_L$ [MPa]	$\langle\sigma_T\rangle$ [MPa]	$\Delta\sigma_T$ [MPa]	$\langle\sigma_L\rangle$ [MPa]	$\Delta\sigma_L$ [MPa]	$\langle\sigma_T\rangle$ [MPa]	$\Delta\sigma_T$ [MPa]
35	600	2	0.05	**-465**	17	**-648**	27	**-289**	18	**-930**	23
35	450	2	0.07	**-502**	14	**-730**	19	**-393**	21	**-858**	22
35	600	3	0.05	**-820**	14	**-776**	15	**-520**	19	**-947**	19
35	600	2	0.07	**-581**	20	**-804**	18	**-479**	18	**-910**	18
20	450	3	0.07	**-402**	15	**-780**	23	**-480**	17	**-1075**	21
20	600	3	0.07	**-306**	14	**-752**	24	**-413**	17	**-920**	24
20	600	2	0.07	**-384**	17	**-641**	24	**-84**	23	**-600**	28
20	600	3	0.05	**-304**	17	**-729**	23	**-368**	18	**-982**	25
35	450	3	0.05	**-588**	18	**-835**	24	**-633**	14	**-991**	23
20	450	2	0.05	**-258**	22	**-712**	24	**-393**	28	**-871**	24
35	450	3	0.07	**-554**	15	**-887**	15	**-637**	20	**-1125**	18

[2] Samples were ground by two cuts (roughing and finishing) or using three cuts (roughing, semi-finishing and finishing).

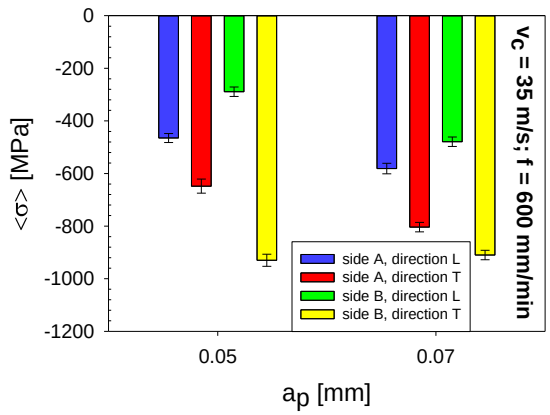

Fig. 9: Average RS on the surface of the both sides and directions depending on the depth of the final cut a_p.

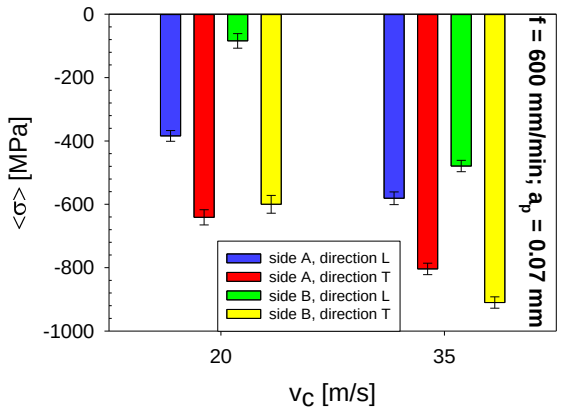

Fig. 10: Average RS on the surface of the both sides and directions depending on the cutting speed v_c.

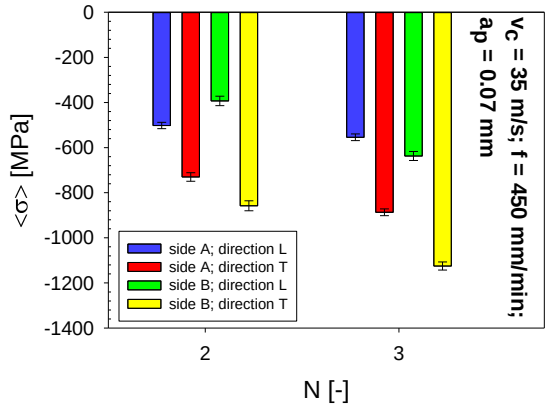

Fig. 11: Average RS on the surface of the both sides and directions depending on the number of cut N.

4 Conclusion

On all ground surfaces of the investigated blade roots, except surfaces with cracks, compressive RS were observed, see Tab. 1. The greater depth of cut, preceding the final cut, led to higher value of macroscopic compressive RS. It is possible to pronounce that greater final depth of cut and higher cutting speeds led to higher compressive RS. Examples of determined results of RS were presented in Figs. 9-11. The drops in compressive RS on the surfaces of several blades were explained by cracks, grinding burns and coarse-grained microstructure of bulk material, see Figs. 6-8.

Acknowledgement

This work was supported by the governmental funding of Technological Agency of Czech Republic – project number TA04010600.

References

[1] W. Österle, P. X. Li, Mechanical and thermal response of a nickel-base superalloy upon grinding with high removal rates, Materials Science and Engineering: A 238.2 (1997) 357-366.

[2] K. Kolařík et al., Non-Destructive Inspection of Surface Integrity in Milled Turbine Blades of Inconel 738LC, Applied Mechanics and Materials 486 (2014) 9-15.

[3] J. Čapek et al., Grinding of Inconel 713 Superalloy for Gas Turbines, Manufacturing Technology 16.1 (2016) 38-45.

[4] J. Li, R. P. Wahi, Investigation of γ/γ′ lattice mismatch in the polycrystalline nickel-base superalloy IN738LC, Acta Metallurgica et Materialia 43 (1995) 507-517.

[5] R. Hill, The elastic behaviour of a crystalline aggregate, in proc.: Proceedings of the Physical Society: A 65.5 (1952) 349.

[6] J. Čapek, Z. Pala, Auxiliary programs for diffraction experiments, Materials Structure 22 (2015) 78-81.

[7] Z. Pala, N. Ganev, J. Drahokoupil, A. Sveshnikov, Surface Layers' Real Structure of Metals Exposed to Inhomogeneous Thermal Fields and Plastic Deformation, Solid State Phenomena 163 (2010) 59-63.

[8] F. Neckář, I. Kvasnička, Vybrané statě z úběru materiálu, Praha, ČVUT, 2011.